arXiv:hep-ex/0303033v1 22 Mar 2003

EUROPEAN ORGANIZATION FOR NUCLEAR RESEARCH

CERN–EP/2002-090

17 December 2002

Search for resonant $\tilde{\nu}$ production at $\sqrt{s} = 183$ to 208 GeV

DELPHI Collaboration

Abstract

Searches for resonant $\tilde{\nu}$ production in e^+e^- collisions under the assumption that R-parity is not conserved and that the dominant R-parity violating coupling is λ_{121} or λ_{131} used data recorded by DELPHI in 1997 to 2000 at centre-of-mass energies of 183 to 208 GeV. No deviation from the Standard Model was observed. Upper limits are given for the λ_{121} and λ_{131} couplings as a function of the sneutrino mass and total width. The limits are especially stringent for sneutrino masses equal to the centre-of-mass energies with the highest integrated luminosities recorded.

(Accepted by E. Phys. J. C)

J.Abdallah[24], P.Abreu[22], W.Adam[50], P.Adzic[11], T.Albrecht[17], T.Alderweireld[2], R.Alemany-Fernandez[8], T.Allmendinger[17], P.P.Allport[23], U.Amaldi[28], N.Amapane[44], S.Amato[47], E.Anashkin[35], A.Andreazza[27], S.Andringa[22], N.Anjos[22], P.Antilogus[26], W-D.Apel[17], Y.Arnoud[14], S.Ask[25], B.Asman[43], J.E.Augustin[24], A.Augustinus[8], P.Baillon[8], A.Ballestrero[45], P.Bambade[20], R.Barbier[26], D.Bardin[16], G.Barker[17], A.Baroncelli[38], M.Battaglia[8], M.Baubillier[24], K-H.Becks[52], M.Begalli[6], A.Behrmann[52], E.Ben-Haim[20], N.Benekos[31], A.Benvenuti[5], C.Berat[14], M.Berggren[24], L.Berntzon[43], D.Bertrand[2], M.Besancon[39], N.Besson[39], D.Bloch[9], M.Blom[30], M.Bluj[51], M.Bonesini[28], M.Boonekamp[39], P.S.L.Booth[23], G.Borisov[21], O.Botner[48], B.Bouquet[20], T.J.V.Bowcock[23], I.Boyko[16], M.Bracko[42], R.Brenner[48], E.Brodet[34], P.Bruckman[18], J.M.Brunet[7], L.Bugge[32], P.Buschmann[52], M.Calvi[28], T.Camporesi[8], V.Canale[37], F.Carena[8], N.Castro[22], F.Cavallo[5], M.Chapkin[41], Ph.Charpentier[8], P.Checchia[35], R.Chierici[8], P.Chliapnikov[41], J.Chudoba[8], S.U.Chung[8], K.Cieslik[18], P.Collins[8], R.Contri[13], G.Cosme[20], F.Cossutti[46], M.J.Costa[49], B.Crawley[1], D.Crennell[36], J.Cuevas[33], J.D'Hondt[2], J.Dalmau[43], T.da Silva[47], W.Da Silva[24], G.Della Ricca[46], A.De Angelis[46], W.De Boer[17], C.De Clercq[2], B.De Lotto[46], N.De Maria[44], A.De Min[35], L.de Paula[47], L.Di Ciaccio[37], A.Di Simone[38], K.Doroba[51], J.Drees[52,8], M.Dris[31], G.Eigen[4], T.Ekelof[48], M.Ellert[48], M.Elsing[8], M.C.Espirito Santo[8], G.Fanourakis[11], D.Fassouliotis[11,3], M.Feindt[17], J.Fernandez[40], A.Ferrer[49], F.Ferro[13], U.Flagmeyer[52], H.Foeth[8], E.Fokitis[31], F.Fulda-Quenzer[20], J.Fuster[49], M.Gandelman[47], C.Garcia[49], Ph.Gavillet[8], E.Gazis[31], T.Geralis[11], R.Gokieli[8,51], B.Golob[42], G.Gomez-Ceballos[40], P.Goncalves[22], E.Graziani[38], G.Grosdidier[20], K.Grzelak[51], J.Guy[36], C.Haag[17], A.Hallgren[48], K.Hamacher[52], K.Hamilton[34], J.Hansen[32], S.Haug[32], F.Hauler[17], V.Hedberg[25], M.Hennecke[17], H.Herr[8], J.Hoffman[51], S-O.Holmgren[43], P.J.Holt[8], M.A.Houlden[23], K.Hultqvist[43], J.N.Jackson[23], G.Jarlskog[25], P.Jarry[39], D.Jeans[34], E.K.Johansson[43], P.D.Johansson[43], P.Jonsson[26], C.Joram[8], L.Jungermann[17], F.Kapusta[24], S.Katsanevas[26], E.Katsoufis[31], G.Kernel[42], B.P.Kersevan[8,42], A.Kiiskinen[15], B.T.King[23], N.J.Kjaer[8], P.Kluit[30], P.Kokkinias[11], C.Kourkoumelis[3], O.Kouznetsov[16], Z.Krumstein[16], M.Kucharczyk[18], J.Lamsa[1], G.Leder[50], F.Ledroit[14], L.Leinonen[43], R.Leitner[29], J.Lemonne[2], V.Lepeltier[20], T.Lesiak[18], W.Liebig[52], D.Liko[50], A.Lipniacka[43], J.H.Lopes[47], J.M.Lopez[33], D.Loukas[11], P.Lutz[39], L.Lyons[34], J.MacNaughton[50], A.Malek[52], S.Maltezos[31], F.Mandl[50], J.Marco[40], R.Marco[40], B.Marechal[47], M.Margoni[35], J-C.Marin[8], C.Mariotti[8], A.Markou[11], C.Martinez-Rivero[40], J.Masik[12], N.Mastroyiannopoulos[11], F.Matorras[40], C.Matteuzzi[28], F.Mazzucato[35], M.Mazzucato[35], R.Mc Nulty[23], C.Meroni[27], W.T.Meyer[1], E.Migliore[44], W.Mitaroff[50], U.Mjoernmark[25], T.Moa[43], M.Moch[17], K.Moenig[8,10], R.Monge[13], J.Montenegro[30], D.Moraes[47], S.Moreno[22], P.Morettini[13], U.Mueller[52], K.Muenich[52], M.Mulders[30], L.Mundim[6], W.Murray[36], B.Muryn[19], G.Myatt[34], T.Myklebust[32], M.Nassiakou[11], F.Navarria[5], K.Nawrocki[51], R.Nicolaidou[39], M.Nikolenko[16,9], A.Oblakowska-Mucha[19], V.Obraztsov[41], A.Olshevski[16], A.Onofre[22], R.Orava[15], K.Osterberg[15], A.Ouraou[39], A.Oyanguren[49], M.Paganoni[28], S.Paiano[5], J.P.Palacios[23], H.Palka[18], Th.D.Papadopoulou[31], L.Pape[8], C.Parkes[23], F.Parodi[13], U.Parzefall[8], A.Passeri[38], O.Passon[52], L.Peralta[22], V.Perepelitsa[49], A.Perrotta[5], A.Petrolini[13], J.Piedra[40], L.Pieri[38], F.Pierre[39], M.Pimenta[22], E.Piotto[8], T.Podobnik[42], V.Poireau[39], M.E.Pol[6], G.Polok[18], P.Poropat[†46], V.Pozdniakov[16], N.Pukhaeva[2,16], A.Pullia[28], J.Rames[12], L.Ramler[17], A.Read[32], P.Rebecchi[8], J.Rehn[17], D.Reid[30], R.Reinhardt[52], P.Renton[34], F.Richard[20], J.Ridky[12], M.Rivero[40], D.Rodriguez[40], A.Romero[44], P.Ronchese[35], E.Rosenberg[1], P.Roudeau[20], T.Rovelli[5], V.Ruhlmann-Kleider[39], D.Ryabtchikov[41], A.Sadovsky[16], L.Salmi[15], J.Salt[49], A.Savoy-Navarro[24], U.Schwickerath[8], A.Segar[34], R.Sekulin[36], M.Siebel[52], A.Sisakian[16], G.Smadja[26], O.Smirnova[25], A.Sokolov[41], A.Sopczak[21], R.Sosnowski[51], T.Spassov[8], M.Stanitzki[17], A.Stocchi[20], J.Strauss[50], B.Stugu[4], M.Szczekowski[51], M.Szeptycka[51], T.Szumlak[19], T.Tabarelli[28], A.C.Taffard[23], F.Tegenfeldt[48], J.Timmermans[30], L.Tkatchev[16], M.Tobin[23], S.Todorovova[12], A.Tomaradze[8], B.Tome[22], A.Tonazzo[28], P.Tortosa[49], P.Travnicek[12], D.Treille[8], G.Tristram[7], M.Trochimczuk[51], C.Troncon[27], M-L.Turluer[39], I.A.Tyapkin[16], P.Tyapkin[16], S.Tzamarias[11], V.Uvarov[41], G.Valenti[5], P.Van Dam[30], J.Van Eldik[8], A.Van Lysebetten[2], N.van Remortel[2], I.Van Vulpen[30], G.Vegni[27], F.Veloso[22], W.Venus[36], F.Verbeure[2], P.Verdier[26], V.Verzi[37], D.Vilanova[39], L.Vitale[46], V.Vrba[12], H.Wahlen[52],

A.J.Washbrook[23], C.Weiser[17], D.Wicke[8], J.Wickens[2], G.Wilkinson[34], M.Winter[9], M.Witek[18], O.Yushchenko[41], A.Zalewska[18], P.Zalewski[51], D.Zavrtanik[42], N.I.Zimin[16], A.Zintchenko[16], M.Zupan[11]

[1]Department of Physics and Astronomy, Iowa State University, Ames IA 50011-3160, USA
[2]Physics Department, Universiteit Antwerpen, Universiteitsplein 1, B-2610 Antwerpen, Belgium
and IIHE, ULB-VUB, Pleinlaan 2, B-1050 Brussels, Belgium
and Faculté des Sciences, Univ. de l'Etat Mons, Av. Maistriau 19, B-7000 Mons, Belgium
[3]Physics Laboratory, University of Athens, Solonos Str. 104, GR-10680 Athens, Greece
[4]Department of Physics, University of Bergen, Allégaten 55, NO-5007 Bergen, Norway
[5]Dipartimento di Fisica, Università di Bologna and INFN, Via Irnerio 46, IT-40126 Bologna, Italy
[6]Centro Brasileiro de Pesquisas Físicas, rua Xavier Sigaud 150, BR-22290 Rio de Janeiro, Brazil
and Depto. de Física, Pont. Univ. Católica, C.P. 38071 BR-22453 Rio de Janeiro, Brazil
and Inst. de Física, Univ. Estadual do Rio de Janeiro, rua São Francisco Xavier 524, Rio de Janeiro, Brazil
[7]Collège de France, Lab. de Physique Corpusculaire, IN2P3-CNRS, FR-75231 Paris Cedex 05, France
[8]CERN, CH-1211 Geneva 23, Switzerland
[9]Institut de Recherches Subatomiques, IN2P3 - CNRS/ULP - BP20, FR-67037 Strasbourg Cedex, France
[10]Now at DESY-Zeuthen, Platanenallee 6, D-15735 Zeuthen, Germany
[11]Institute of Nuclear Physics, N.C.S.R. Demokritos, P.O. Box 60228, GR-15310 Athens, Greece
[12]FZU, Inst. of Phys. of the C.A.S. High Energy Physics Division, Na Slovance 2, CZ-180 40, Praha 8, Czech Republic
[13]Dipartimento di Fisica, Università di Genova and INFN, Via Dodecaneso 33, IT-16146 Genova, Italy
[14]Institut des Sciences Nucléaires, IN2P3-CNRS, Université de Grenoble 1, FR-38026 Grenoble Cedex, France
[15]Helsinki Institute of Physics, HIP, P.O. Box 9, FI-00014 Helsinki, Finland
[16]Joint Institute for Nuclear Research, Dubna, Head Post Office, P.O. Box 79, RU-101 000 Moscow, Russian Federation
[17]Institut für Experimentelle Kernphysik, Universität Karlsruhe, Postfach 6980, DE-76128 Karlsruhe, Germany
[18]Institute of Nuclear Physics,Ul. Kawiory 26a, PL-30055 Krakow, Poland
[19]Faculty of Physics and Nuclear Techniques, University of Mining and Metallurgy, PL-30055 Krakow, Poland
[20]Université de Paris-Sud, Lab. de l'Accélérateur Linéaire, IN2P3-CNRS, Bât. 200, FR-91405 Orsay Cedex, France
[21]School of Physics and Chemistry, University of Lancaster, Lancaster LA1 4YB, UK
[22]LIP, IST, FCUL - Av. Elias Garcia, 14-1^{o}, PT-1000 Lisboa Codex, Portugal
[23]Department of Physics, University of Liverpool, P.O. Box 147, Liverpool L69 3BX, UK
[24]LPNHE, IN2P3-CNRS, Univ. Paris VI et VII, Tour 33 (RdC), 4 place Jussieu, FR-75252 Paris Cedex 05, France
[25]Department of Physics, University of Lund, Sölvegatan 14, SE-223 63 Lund, Sweden
[26]Université Claude Bernard de Lyon, IPNL, IN2P3-CNRS, FR-69622 Villeurbanne Cedex, France
[27]Dipartimento di Fisica, Università di Milano and INFN-MILANO, Via Celoria 16, IT-20133 Milan, Italy
[28]Dipartimento di Fisica, Univ. di Milano-Bicocca and INFN-MILANO, Piazza della Scienza 2, IT-20126 Milan, Italy
[29]IPNP of MFF, Charles Univ., Areal MFF, V Holesovickach 2, CZ-180 00, Praha 8, Czech Republic
[30]NIKHEF, Postbus 41882, NL-1009 DB Amsterdam, The Netherlands
[31]National Technical University, Physics Department, Zografou Campus, GR-15773 Athens, Greece
[32]Physics Department, University of Oslo, Blindern, NO-0316 Oslo, Norway
[33]Dpto. Fisica, Univ. Oviedo, Avda. Calvo Sotelo s/n, ES-33007 Oviedo, Spain
[34]Department of Physics, University of Oxford, Keble Road, Oxford OX1 3RH, UK
[35]Dipartimento di Fisica, Università di Padova and INFN, Via Marzolo 8, IT-35131 Padua, Italy
[36]Rutherford Appleton Laboratory, Chilton, Didcot OX11 OQX, UK
[37]Dipartimento di Fisica, Università di Roma II and INFN, Tor Vergata, IT-00173 Rome, Italy
[38]Dipartimento di Fisica, Università di Roma III and INFN, Via della Vasca Navale 84, IT-00146 Rome, Italy
[39]DAPNIA/Service de Physique des Particules, CEA-Saclay, FR-91191 Gif-sur-Yvette Cedex, France
[40]Instituto de Fisica de Cantabria (CSIC-UC), Avda. los Castros s/n, ES-39006 Santander, Spain
[41]Inst. for High Energy Physics, Serpukov P.O. Box 35, Protvino, (Moscow Region), Russian Federation
[42]J. Stefan Institute, Jamova 39, SI-1000 Ljubljana, Slovenia and Laboratory for Astroparticle Physics,
Nova Gorica Polytechnic, Kostanjeviska 16a, SI-5000 Nova Gorica, Slovenia,
and Department of Physics, University of Ljubljana, SI-1000 Ljubljana, Slovenia
[43]Fysikum, Stockholm University, Box 6730, SE-113 85 Stockholm, Sweden
[44]Dipartimento di Fisica Sperimentale, Università di Torino and INFN, Via P. Giuria 1, IT-10125 Turin, Italy
[45]INFN,Sezione di Torino, and Dipartimento di Fisica Teorica, Università di Torino, Via P. Giuria 1,
IT-10125 Turin, Italy
[46]Dipartimento di Fisica, Università di Trieste and INFN, Via A. Valerio 2, IT-34127 Trieste, Italy
and Istituto di Fisica, Università di Udine, IT-33100 Udine, Italy
[47]Univ. Federal do Rio de Janeiro, C.P. 68528 Cidade Univ., Ilha do Fundão BR-21945-970 Rio de Janeiro, Brazil
[48]Department of Radiation Sciences, University of Uppsala, P.O. Box 535, SE-751 21 Uppsala, Sweden
[49]IFIC, Valencia-CSIC, and D.F.A.M.N., U. de Valencia, Avda. Dr. Moliner 50, ES-46100 Burjassot (Valencia), Spain
[50]Institut für Hochenergiephysik, Österr. Akad. d. Wissensch., Nikolsdorfergasse 18, AT-1050 Vienna, Austria
[51]Inst. Nuclear Studies and University of Warsaw, Ul. Hoza 69, PL-00681 Warsaw, Poland
[52]Fachbereich Physik, University of Wuppertal, Postfach 100 127, DE-42097 Wuppertal, Germany
† deceased

1 Introduction

In the Minimal Supersymmetric extension of the Standard Model (MSSM) [1], a discrete symmetry called R-parity [2] predicts baryon number (B) and lepton number (L) conservation which is an accidental feature of the SU(3)×SU(2)×U(1) Standard Model (SM). The related quantum number $R_p = (-1)^{3B+L+2S}$, where S is the spin of the particle, is multiplicatively conserved. However, from a theoretical point of view, R-parity conservation is not needed. Allowing its violation leads to a more general superpotential W which can include the following renormalizable gauge invariant additional terms:

$$W_{\Delta L\neq 0} = \lambda_{ijk} L_i L_j \bar{E}_k + \lambda'_{ijk} L_i Q_j \bar{D}_k + \epsilon_i H_u L_i$$

$$W_{\Delta B\neq 0} = \lambda''_{ijk} \bar{U}_i \bar{D}_j \bar{D}_k.$$

Here L (Q) are the lepton (quark) doublet superfields, $\bar{E}$ ($\bar{U}$, $\bar{D}$) are the lepton (up and down quark) singlet superfields, H_u is the Higgs superdoublet coupling to up-type quarks and leptons, i, j, k are generation indices; ϵ_i are parameters with dimensions while λ_{ijk}, λ'_{ijk}, λ''_{ijk} are dimensionless Yukawa-like couplings. The λ_{ijk} (λ''_{ijk}) couplings are anti-symmetric in the first (last) two indices because of gauge invariance.

Nevertheless, it is necessary to require that $\Delta L \neq 0$ and $\Delta B \neq 0$ terms are not both present to avoid a fast proton decay. In this paper, it will be assumed that only one λ_{ijk} coupling is non-vanishing.

R-parity violation has two major consequences. It allows the decay of the lightest supersymmetric particle (LSP), thus discarding it as a candidate to cold dark matter. It also allows the supersymmetric particles to be singly produced, via λ_{ijk} couplings in the case of e^+e^- collisions. It is this possibility that is explored in this paper. If λ_{121} or λ_{131} is non-vanishing, a muon sneutrino or a tau sneutrino (an electron sneutrino cannot be produced because $\lambda_{111} = 0$), with spin 0, can be produced in the s-channel [3] (see Figure 1). The simplest expression for the cross-section is [4]:

$$\sigma(e^+e^- \to \tilde{\nu} \to X)(s) = \frac{4\pi s}{M^2_{\tilde{\nu}}} \frac{\Gamma(ee)\Gamma(X)}{(s - M^2_{\tilde{\nu}})^2 + M^2_{\tilde{\nu}}\Gamma^2_{\tilde{\nu}}}$$

where $\Gamma(ee) = \Gamma(\tilde{\nu}_j \to e^+e^-) = \dfrac{\lambda^2_{1j1}}{16\pi} M_{\tilde{\nu}}$, $j = 2, 3$ and $\Gamma(X)$ denotes the partial width for $\tilde{\nu}_j$ decay to a final state X, with $X = e^+e^-$ (sneutrino direct decay), $\tilde{\chi}^0\nu$ or $\tilde{\chi}^{\pm}l^{\mp}$ (sneutrino indirect decays). In the indirect decay mode, $\Gamma(X)$ is independent of λ_{1j1}. The additional t-channel contributions and the interference terms, not shown in this formula for reasons of compactness, were included in the signal simulation [5] and final estimation of expected events. This cross-section is expected to be very high for $M_{\tilde{\nu}} \simeq \sqrt{s}$ (of the order of 50 pb for instance for $\lambda_{1j1} = 10^{-2}$) and to remain large for masses below the centre-of-mass energy, due to initial state radiation effects, again not displayed by this formula but taken into account in the analysis.

Given the present (indirect) upper limits on λ_{121} and λ_{131} ($\lambda_{121} < 0.04 \times \frac{M_{\tilde{e}_R}}{100\ \mathrm{GeV}/c^2}$, $\lambda_{131} < 0.05 \times \frac{M_{\tilde{e}_R}}{100\ \mathrm{GeV}/c^2}$ at 68% confidence level (CL) [6]), the e^+e^- decay channel, having a cross-section proportional to λ^4, is suppressed compared to the other two ($\sigma \propto \lambda^2$), unless all neutralinos and charginos are heavier than the sneutrino. The direct decay mode has already been investigated by the LEP collaborations [7] by looking for deviations from the Standard Model in the cross-sections and asymmetries of $e^+e^- \to l^+l^-$. The results were presented as an upper limit on λ_{1j1} as a function of the sneutrino mass $M_{\tilde{\nu}}$. The indirect decay modes are analysed explicitly here, taking into account any mass and width of the

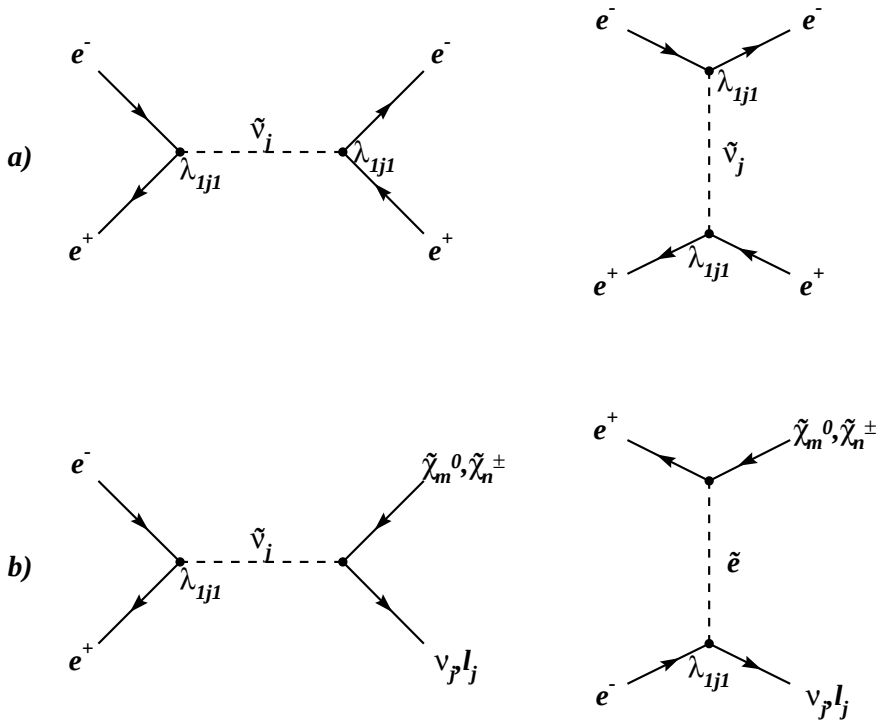

Figure 1: Lowest order Feynman diagrams for single sneutrino production and decay: a) direct decay, b) indirect decay ($\nu_j = \nu_\mu, \nu_\tau$; $l_j = \mu, \tau$; m = 1,4; n = 1,2).

sneutrino as a function of the MSSM parameters. The scheme chosen here is a constrained MSSM in which the SUSY breaking occurs via gravitational interactions (mSUGRA [1]). The relevant parameters are then: M_2, the SU(2) gaugino mass at the electroweak scale; m_0, the scalars common mass at the Grand Unified Theories (GUT) scale; μ, the mixing mass term of the Higgs doublets at the electroweak scale; and $\tan\beta$, the ratio of the vacuum expectation values of the two Higgs doublets. The unified trilinear coupling A_0 is assumed to be zero. It is also assumed that the running of the λ couplings from the GUT scale to the electroweak scale does not have a significant effect on the running of the gaugino and sfermion masses.

In this model, the LSP is generally the lightest neutralino $\tilde{\chi}_1^0$; with a λ_{121} (λ_{131}) coupling, it decays to $e\mu\nu_e$ or $ee\nu_\mu$ ($e\tau\nu_e$ or $ee\nu_\tau$). All other sparticles, like the sneutrino, can have both direct and indirect decays. In particular, the lightest chargino $\tilde{\chi}_1^+$ can decay either to $ee\mu$, $e\nu_e\nu_\mu$ (λ_{121}) or to the R_p conserving channel $\tilde{\chi}_1^0 W^\star$. The latter is generally clearly dominant over the former, unless the λ coupling is very large or the mass difference between the chargino and the neutralino is very small. The decays of the heavier neutralinos and charginos are similar, with the additional possibility of longer cascade decays always leading to the LSP decay.

A complete review of the possible decays of the neutralinos and charginos showed that the final states of all indirect decays of the sneutrino could be classified into three topologies (or channels):

1) events with two leptons and missing energy;
2) events with four or six leptons (with or without missing energy);
3) events with at least two isolated leptons and at least two hadronic jets.

The first topology mostly comes from $\tilde{\nu} \to \tilde{\chi}_1^0\nu$, $\tilde{\chi}_1^0 \to e^\pm l^\mp \nu$, leading to a $2l + \nu$ final state. The second one is dominated by $\tilde{\nu} \to \tilde{\chi}_1^+ l^-$, $\tilde{\chi}_1^+ \to \tilde{\chi}_1^0 l^+\nu$, $\tilde{\chi}_1^0 \to e^\pm l^\mp \nu$, leading to $4l + 2\nu$. The third topology, being relatively general, often has a high branching ratio. It can arise for example from $\tilde{\nu} \to \tilde{\chi}_1^+ l^-$, $\tilde{\chi}_1^+ \to \tilde{\chi}_1^0 q\bar{q}'$, $\tilde{\chi}_1^0 \to e^\pm l^\mp \nu$, leading to $3l + 2\text{jets}+\nu$, or from $\tilde{\nu} \to \tilde{\chi}_2^0\nu$, $\tilde{\chi}_2^0 \to \tilde{\chi}_1^0 q\bar{q}$, $\tilde{\chi}_1^0 \to e^\pm l^\mp \nu$, leading to $2l + 2\text{jets}+2\nu$.

The paper is organised as follows. Section 2 lists the data samples that were used in the present search for resonant sneutrino production. In section 3, the selection criteria are described, as well as the results of the selection. Finally, in section 4 the limits on the λ_{1j1} couplings are derived by comparing the Standard Model expectations and the experimental results.

2 Data samples

A detailed description of the DELPHI detector can be found in [8]. The present analysis was mainly based on the capability of reconstructing charged particle tracks using the tracking devices, particularly the Time Projection Chamber (TPC) but also the silicon Vertex Detector, the drift chambers called Inner and Outer Detectors, and the forward detectors. The complete system was inside a solenoidal magnetic field of 1.2 T, parallel to the beam axis. The analysis also used the lepton identification capabilities of the electromagnetic calorimeters (the barrel High density Projection Chamber HPC and the Forward Electro-Magnetic Calorimeter FEMC) for the electrons and of the muon chambers for the muons. The hadron calorimeter was used to detect neutral hadrons.

The data from 1997 to 2000 LEP runs were taken at centre-of-mass energies between 183 GeV and 208 GeV. The registered integrated luminosities after requiring the TPC

$<\sqrt{s}>$(GeV)	$\int\mathcal{L}$ (pb^{-1})
182.7	52.2
188.6	153.8
191.6	25.1
195.5	75.9
199.5	82.8
201.6	43.2
203.7	6.3
205.0	67.2
206.5	78.2
208.0	7.3
All	592.0

Table 1: Average centre-of-mass energies and integrated luminosities.

and all the calorimeters (HPC, FEMC and hadron calorimeter) to be operational are given in Table 1. This quality requirement rejected 2% of the luminosity recorded in 1997 to 1999 and 29% of 2000 integrated luminosity, because one of the twelve sectors of the TPC was off before the end of the data taking. Runs with partly inefficient muon chambers were kept, and the simulation was adjusted to reproduce the effective efficiency.

To evaluate the background contamination, different contributions coming from the Standard Model were considered. The Standard Model events were produced by the following generators: `BDKRC` [9] for the $e^+e^- \to e^+e^-l^+l^-$ four-fermion events of type $\gamma\gamma$, and `WPHACT` [10] for the other four-fermion events; `KK2F` [11] for the two-fermion events of type $e^+e^- \to f\bar{f}(\gamma)$, with $f \neq e$, τ, `BHWIDE` [12] for the Bhabha events ($f = e$) and `KORALZ` [13] for $f = \tau$ events; `PYTHIA` [14] and `WPHACT` for the $\gamma\gamma \to$ hadrons events.

Signal events were generated with the `SUSYGEN 2.20` generator [5]. Samples of 3500 to 6000 events were generated for nine MSSM parameter sets (see Table 2).

Simulated events were produced from the generated samples with the standard DELPHI simulation program `DELSIM` [8] and passed through the same reconstruction chain as the data. These events were used to design the event selection.

A faster simulation programme (`SGV`) [15] was applied to the same generated samples in order to be validated for further use in the limits extraction.

3 Event selection

In order to select the three categories of final states defined above, a preselection was first applied. In the following, charged particles reconstructed from their trajectories in the tracking chambers were accepted only if their momenta were greater than 100 MeV/c and less than 1.5 times the beam energy. They also had to have a relative momentum error less than 100% and impact parameters of at most 4 cm both in the plane transverse to the beam and along the beam direction. On the other hand, a neutral particle is assumed to be detected as a cluster of energy deposits not associated to a track. In each event, the following were required:

- at least two charged particles;

Parameter set	m_0	μ	M_2	$\Gamma_{\tilde{\nu}}$	m($\tilde{\chi}_1^0$)	m($\tilde{\chi}_1^+$)	Br_1	Br_2	Br_3
1	150	175	125	1	37	68	0.39	0.23	0.38
2	190	275	155	1	65	116	0.42	0.24	0.34
3	200	195	175	1	64	106	0.41	0.20	0.38
4	207	125	385	0.2	87	104	0.57	0.15	0.28
5	207	-75	155	0.5	71	96	0.19	0.24	0.57
6	207	-125	115	1	63	127	0.10	0.17	0.72
7	207	305	135	1.5	57	105	0.37	0.24	0.39
8	207	-285	65	2	36	81	0.17	0.37	0.46
9	220	285	185	1	80	142	0.52	0.18	0.31

Table 2: Values of the SUSY parameters (in GeV/c^2) used in the signal simulation, and resulting width, masses and branching ratios (Br_i is the branching ratio of channel number i).

- the sum of all charged particle energies greater than $0.1 \times \sqrt{s}$ (and in any case, total energy of all particles E_{tot} greater than 20 GeV);
- the total momentum transverse to the beam greater than 5 GeV/c;
- the absolute value of total electric charge at most 1 if there are less than 7 charged particles;
- at least one charged particle in the barrel (polar angle between 40° and 140°);
- the absolute value of the cosine of the polar angle of the missing momentum vector below 0.95 (or 0.9 in case of exactly two charged particles);
- at least one isolated (i.e. with no other track in a 5° half-cone centred on its direction) identified lepton (electron or muon) with momentum above 5 GeV/c and with a maximum angle of 170° with respect to the nearest track.

The lepton identification used standard DELPHI tools [8]. The electron identification algorithm relied on two types of informations: the energy deposited in the electromagnetic calorimeters and the dE/dx measurement in the TPC. The muon identification algorithm was based on the association of signals in the muon chambers with extrapolated tracks; the most efficient set of criteria, as described in [8], was chosen for this analysis.

The above criteria define the preselection. Then four more series of requirements were designed, in order to select the different kinds of topologies. For the two acoplanar[1] lepton and four or six lepton topologies, the criteria were the same for both λ_{121} and λ_{131} couplings; for the semi-leptonic topology, two slightly different selections were applied.

- For the two acoplanar lepton final states, it was required that:
  - there be exactly two charged particles;
  - not both identified as muons;
  - the acoplanarity be above 40°;
  - the acollinearity[2] be above 50°;
  - the invariant mass of the two leptons[3] be lower than $0.25 \times \sqrt{s}$;
  - the angle between the two leptons be lower than 100°.

[1]The acoplanarity is 180° minus the angle between the transverse momenta of the two charged particles, or of the two reconstructed jets (forcing the number of jets to be two with the LUCLUS algorithm [16]) if the event contains more particles.

[2]The acollinearity is 180° minus the angle between the two charged particles (or the two jets, see the definition of acoplanarity).

[3]When the second lepton was not identified, it was assumed to be an electron.

- For the four or six lepton final states, the requirements were:
  - four or six charged particles;
  - at least two identified leptons (electrons or muons);
  - the resolution parameter of the Durham algorithm [17] for which the event changes from four to three jets y_{34} greater than 10^{-4}.
- For the semi-leptonic final states, λ_{121} coupling:
  - at least 7 charged particles and at most 25;
  - at least two identified leptons (electrons or muons);
  - the transverse momentum of the second most energetic lepton had to be above $0.05 \times \sqrt{s}$;
  - y_{34} had to be greater than 10^{-3};
  - when the number of jets was forced to four, at least two of them were required to be thin, that is to have a total (track + neutral) multiplicity not exceeding 4.
- For the semi-leptonic final states, λ_{131} coupling:
  - at least 7 charged particles and at most 25;
  - at least two identified leptons (electrons or muons), including at least one identified electron;
  - y_{34} had to be greater than 10^{-3};
  - when the number of jets was forced to four, at least two of them were required to be thin;
  - the missing energy ($\sqrt{s} - E_{tot}$) had to be greater than $0.25 \times \sqrt{s}$.

The numbers of data and of SM Monte Carlo events after the preselection are shown in Table 3. Distributions of some important variables are shown in Figures 2 and 3 at the preselection level. The plots were chosen so as to give at least an example of each centre-of-mass energy. The agreement between real data and simulated SM background is good.

Some examples of signal distributions are also given, for the following parameters: $\lambda_{1j1} = 0.05$, $m_0 = \sqrt{s}$, $\tan\beta = 1.5$, $\mu = -125$ GeV/c^2, $M_2 = 115$ GeV/c^2. The missing energy signal is given for the semi-leptonic channel, $j = 3$, and scaled by a factor of 5; the second lepton transverse momentum and the thin jet multiplicity signals are given for the semi-leptonic channel, $j = 2$, and scaled by a factor of 5 and 2 respectively; the $\log_{10} y_{34}$ signal is given for the four-lepton channel, $j = 3$, and scaled by a factor of 20; the acollinearity and the two-lepton angle signals are given for the two-lepton channel, $j = 2$, and scaled by a factor of 20; the acoplanarity and the two-lepton invariant mass signals are given for the two-lepton channel, $j = 3$, and scaled by a factor of 20 and 50 respectively.

The efficiency of the selections, including the preselection, depends on the SUSY parameters. It is shown in Figure 4 for the nine parameter sets which were fully simulated with `DELSIM` (Table 2) using a λ_{121} coupling and $\sqrt{s} = 206.5$ GeV. The Figure also shows the efficiencies evaluated with `SGV`; they are compatible. The fact that `SGV` efficiencies were systematically lower than `DELSIM` efficiencies in the four or six lepton channel was not compensated for, first because this has a small impact on the global efficiency and second because it gives conservative results. The efficiencies for a λ_{131} coupling are comparable, although always lower.

The expected background at the end of the selections is mainly composed of four-fermion events. The $\gamma\gamma$ background is totally negligible. The background coming from the two-fermion events is small and its proportion decreases when the centre-of-mass

$\sqrt{s}$ (GeV)	SM	Data
182.7	1003±11	1071
188.6	2909±16	2913
191.6	466±3	484
195.5	1387±8	1466
199.5	1487±8	1537
201.6	772±5	777
203.7	110±1	99
205.0	1180±7	1210
206.5	1345±6	1322
208.0	126±1	115

Table 3: Number of events after the preselection (SM= Monte Carlo simulated SM background normalised to the data luminosity). Errors are statistical only.

energy increases. For instance, it is 9% in the two-lepton channel at 183 GeV and 4% at 206.5 GeV.

The number of data and of SM Monte Carlo events at the end of the selections is shown in Table 4. There is no significant excess of data in any of the three channels and in any of the centre-of-mass energy samples.

4 Limits on λ_{121} and λ_{131} couplings

Besides being used as an event generator, `SUSYGEN` was also used to scan a wide part of the MSSM parameter space and compute all the cross-sections of the signal, with $\lambda_{1j1} = 5 \times 10^{-3}$. In the model adopted for this search and described in section 1, all SUSY phenomenology can be derived from the four parameters $\tan\beta$, m_0, M_2 and μ, plus the centre-of-mass energy for the kinematics. The parameter sets explored in the scan were:

- $\sqrt{s} = 182.7$, 188.6, 199.5 and 206.5 GeV,
- $\tan\beta = 1.5$ or 30,
- m_0= 100 to 230 GeV/c^2 (170 to 215 GeV/c^2 in steps of 1 GeV/c^2, 100 to 170 GeV/c^2 in steps of 10 GeV/c^2, 215 to 230 GeV/c^2 in steps of 5 GeV/c^2),
- $M_2 = 5$ to 405 GeV/c^2 in steps of 10 GeV/c^2,
- $\mu = -305$ to 305 GeV/c^2 in steps of 10 GeV/c^2.

The cross-sections at $\sqrt{s} = 191.6$ GeV were taken from the $\sqrt{s} = 188.6$ GeV scan simply assuming $\sqrt{s}+3$ GeV; in the same way, the cross-sections at 195.5 and 201.6 GeV were taken from the 199.5 GeV scan and the cross-sections at 203.7, 205.0 and 208.0 GeV were taken from the 206.5 GeV scan assuming the corresponding centre-of-mass energy shifts.

The sneutrino mass $M_{\tilde{\nu}}$ was assigned the value of m_0, thus slightly departing from a strict mSUGRA model. This is a conservative hypothesis since the sneutrino mass tends to decrease whereas the gaugino masses are left untouched.

Very small values of the sneutrino total width ($\Gamma_{\tilde{\nu}} < 150$ MeV/c^2) correspond to regions of the parameter space where the sneutrino is lighter than the gauginos; they can

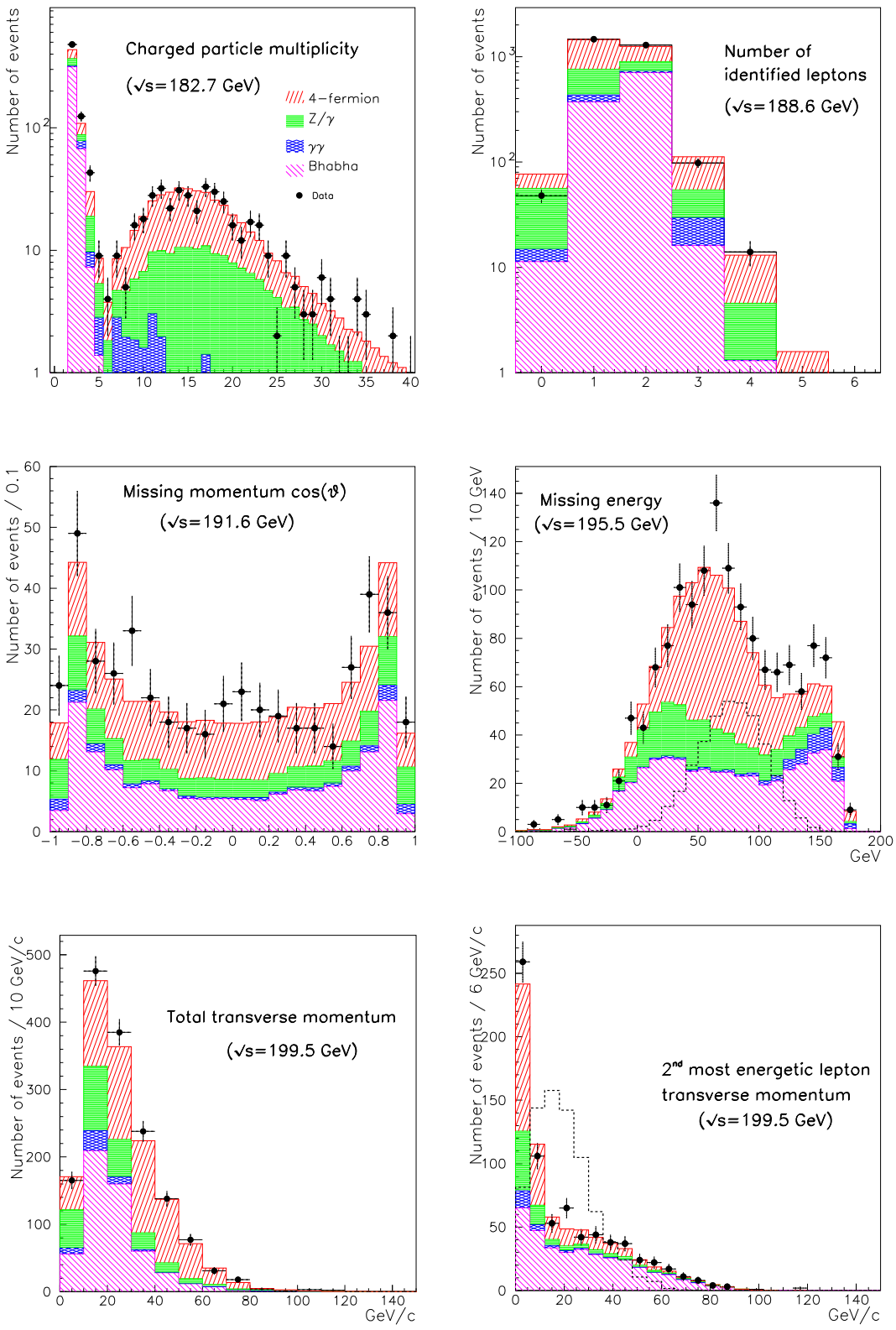

Figure 2: Examples of data-simulation comparison at preselection level. The dashed lines are examples of signal distributions (see text).

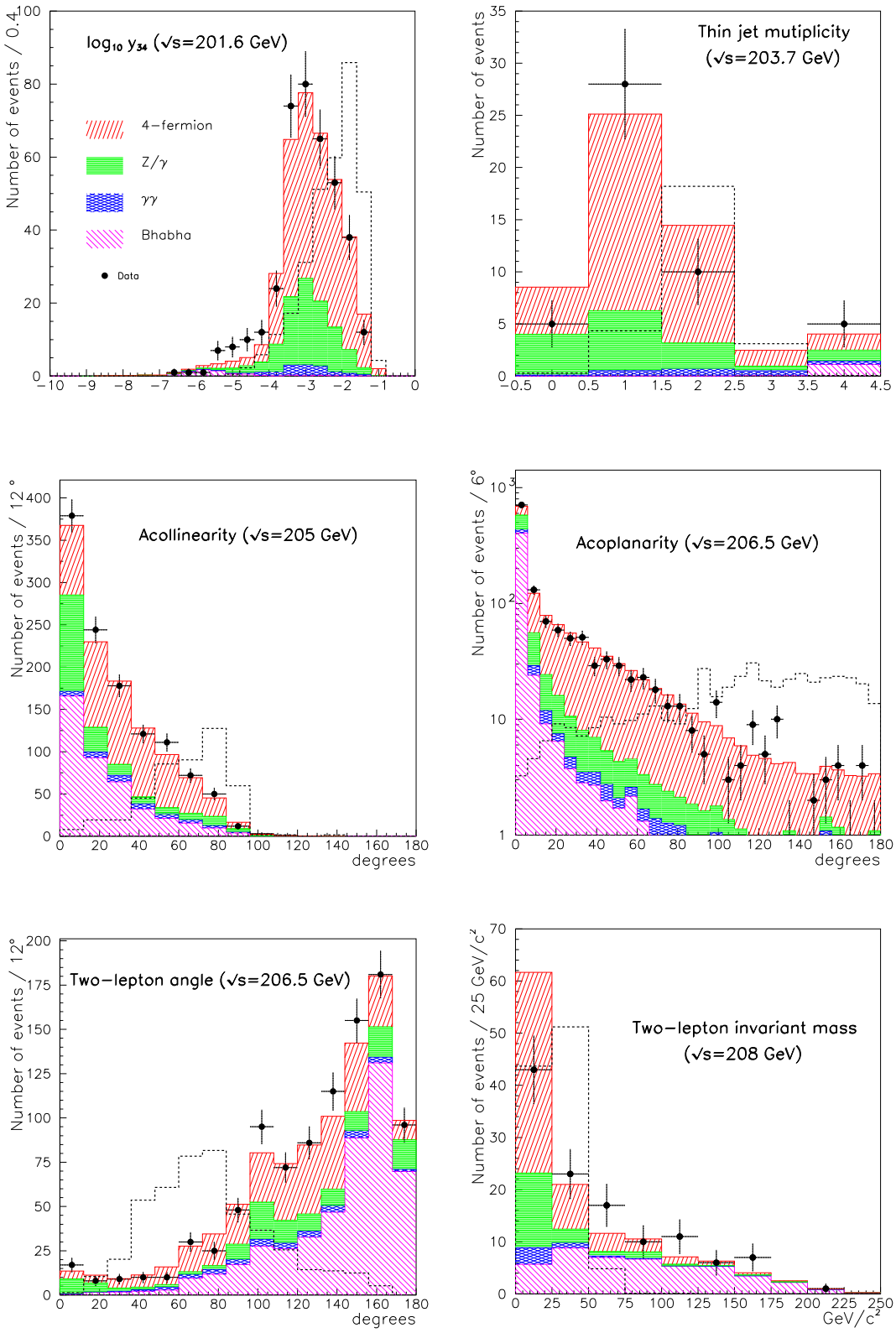

Figure 3: Additional examples of data-simulation comparison at preselection level (the $\log_{10} y_{34}$ and jet multiplicity distributions are given for events with at least four charged particles). The dashed lines are examples of signal distributions (see text).

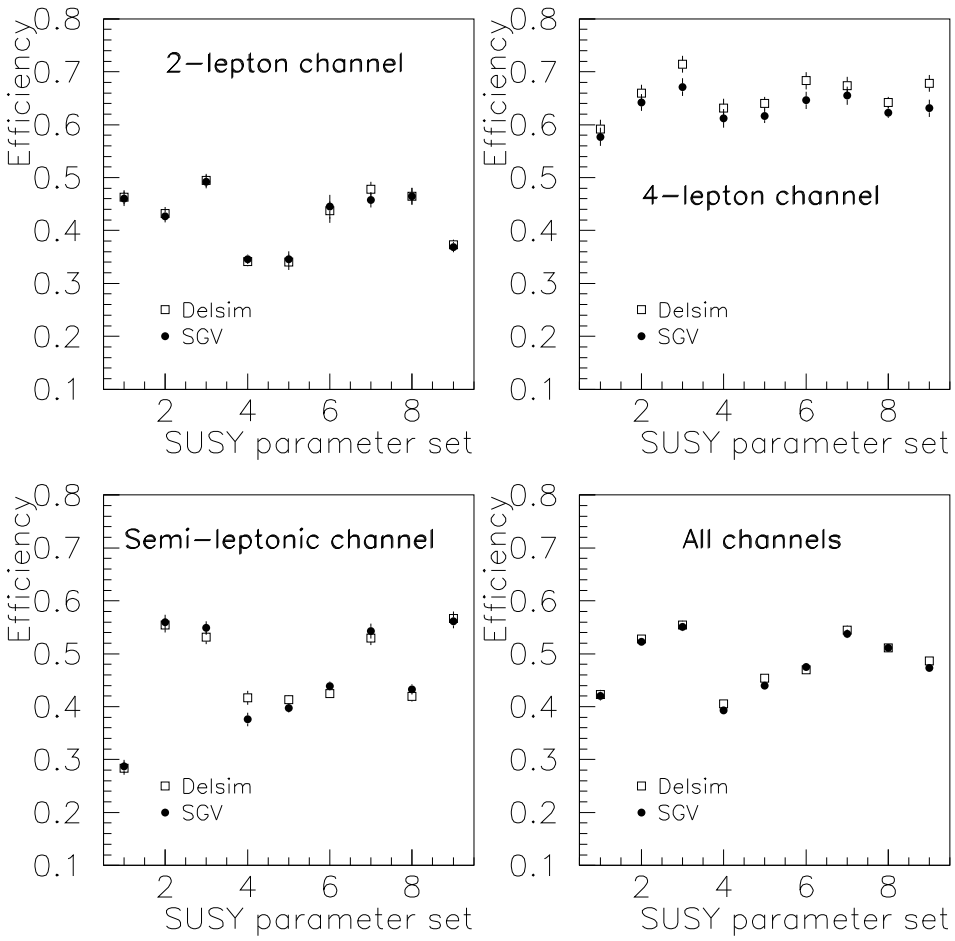

Figure 4: `SGV-DELSIM` comparison for nine SUSY parameter sets with different sneutrino masses and total widths (see Table 2) in the case of a λ_{121} coupling and for $\tan\beta = 1.5$, $\sqrt{s} = 206.5$ GeV. For this comparison, the same number of events was simulated with SGV and DELSIM.

$\sqrt{s}$	(GeV)	2 leptons	4 leptons	semi-leptonic		all channels	
				λ_{121}	λ_{131}	λ_{121}	λ_{131}
182.7	SM	9.3±0.5	3.0±0.3	2.0±0.1	2.5±0.1	14.3±0.6	14.8±0.6
	Data	7	2	4	0	13	9
188.6	SM	26.0±0.5	8.4±0.4	7.3±0.2	7.5±0.2	41.7±0.7	41.9±0.7
	Data	26	7	8	2	41	35
191.6	SM	4.1±0.1	1.5±0.1	1.31±0.03	1.24±0.03	6.9±0.2	6.8±0.2
	Data	2	2	2	2	6	6
195.5	SM	11.9±0.2	3.9±0.2	4.2±0.1	3.7±0.1	20.0±0.3	19.5±0.3
	Data	10	5	5	2	20	17
199.5	SM	13.0±0.3	4.4±0.2	4.8±0.1	4.0±0.1	22.2±0.4	21.4±0.4
	Data	11	4	5	2	20	17
201.6	SM	6.3±0.1	2.2±0.1	2.5±0.1	1.9±0.1	11.0±0.2	10.4±0.2
	Data	3	1	3	3	7	7
203.7	SM	0.93±0.03	0.34±0.02	0.39±0.02	0.30±0.02	1.6±0.1	1.5±0.1
	Data	0	0	0	0	0	0
205.0	SM	10.1±0.3	3.5±0.2	3.9±0.2	3.2±0.2	17.5±0.4	16.8±0.4
	Data	14	4	4	3	22	21
206.5	SM	11.4±0.3	4.4±0.2	4.7±0.3	3.6±0.3	20.5±0.5	19.4±0.5
	Data	12	1	7	3	20	16
208.0	SM	1.04±0.02	0.44±0.04	0.50±0.03	0.36±0.03	1.9±0.1	1.8±0.1
	Data	1	0	0	0	1	1

Table 4: Number of events at the end of the selection (SM = Monte Carlo simulated SM background). Errors are statistical only. Note that the sum of all channels is not independent for λ_{121} and λ_{131} due to the common analysis for the first two channels.

hardly be detected by the present analysis, however they are covered by $e^+e^- \to l^+l^-$ analyses [7].

Regions of the parameter space already excluded by the precision measurements at LEP1 were not further explored in the present scans. This condition was implemented in the following way. Using the expression for the cross-section at the resonance, $\sigma(e^+e^- \to Z \to X) = 12\pi\frac{\Gamma_{ee}\Gamma_X}{M_Z^2\Gamma_Z^2}$, the limit $\Gamma^{\rm new} < 6.6$ MeV/c^2 at 95% CL [18] can be converted into an upper limit on the cross-section of new decay modes: $\sigma^{\rm new} < 157.2$ pb at 95% CL. SUSY parameter sets for which the total cross-section of pair production of charginos and neutralinos at $\sqrt{s} \simeq M_Z$ was larger than this limit were considered as excluded by LEP1.

To derive the limits on one λ coupling, each centre-of-mass energy was first considered separately. The three channels being totally independent due to the charged particle multiplicity criterion, they were summed up (Table 4). On the other hand, the $(M_{\tilde{\nu}}, \Gamma_{\tilde{\nu}})$ plane was divided into rectangular bins of size (1 GeV/c^2, 50 MeV/c^2). For each set of parameters entering a given bin, the output of two scans was used. First the `SUSYGEN` scan to get σ, the total cross-section expected for $e^+e^- \to \tilde{\nu} \to X$, X representing all final states from indirect sneutrino decays. From the expression given in the introduction, $\sigma = \sigma_0 \times \lambda^2$. σ_0 is almost independent of λ as long as λ is reasonably small: for $\lambda = 0.1$, σ_0 is at most a few percent lower than for $\lambda = 10^{-4}$. Second a `SGV` scan on the same

parameters (however with wider steps, of 10 GeV on the full m_0 range and of 20 GeV for μ and M_2), to obtain the global efficiency of the analysis, ϵ, combining the three separate channel efficiencies according to the branching ratios predicted by SUSYGEN. 1000 events were simulated for each parameter set.

An upper limit at 95% CL on the total number of signal events (N_{up}) compatible with the data and expected background was then calculated for each $(M_{\tilde{\nu}}, \Gamma_{\tilde{\nu}})$ bin, combining the ten centre-of-mass energy samples considered as independent samples. This was done using the Bayesian method described in reference [19]; the relative probabilities of each centre-of-mass energy were taken as

$$w_i = \frac{(\sigma_0\epsilon)_i \int \mathcal{L}_i}{\sum_{j=1}^{10} (\sigma_0\epsilon)_j \int \mathcal{L}_j},$$

where $(\sigma_0\epsilon)_i$ is the lowest value of such a product in the considered bin and $\int \mathcal{L}_i$ is the integrated luminosity of the i^{th} sample. The 95% CL upper limit on λ in each bin was then

$$\lambda < \sqrt{\frac{N_{up}}{\sum_{j=1}^{10} (\sigma_0\epsilon)_j \int \mathcal{L}_j}}.$$

The whole procedure was repeated for the second coupling.

The results are shown in Figures 5 to 8 corresponding to the two values of $\tan\beta$ considered. In a very large fraction of the $(M_{\tilde{\nu}}, \Gamma_{\tilde{\nu}})$ plane the obtained upper limit on λ_{1j1} is at most 0.1, and below 0.01 in still the major part of the area allowed by the parameters range.

There are two main sources of systematic errors on these results. One is the estimation of the expected SM background. Uncertainties arise from the Monte Carlo statistics (at most $\pm 5\%$, see Table 4), from the detector response simulation and from the cross-sections evaluation and event modelling. In the last case, a comparison of different generators gave at most $\pm 5\%$ difference, mainly coming from the hadronisation modelling, for the four-fermion processes which are the dominant background. This uncertainty is smaller for two-fermion processes and larger for $\gamma\gamma$ events, which however do not affect the final results because very few events of that kind remain at the end of the selection. The resulting systematic uncertainty on the limit on λ, evaluated separately for each centre-of-mass energy, is of the order of $\pm 2\%$. The second source of systematic errors is the estimation of the selection efficiency, performed with a fast simulation and however statistically limited (up to $\pm 5\%$ on low branching ratio channels). Here an important uncertainty arises from the track reconstruction and the lepton identification efficiencies. Discrepancies between DELSIM and SGV are at the level of $\pm 4\%$ for the global efficiency (Figure 4). The resulting variation of the limit on λ, using the prescription of reference [20], is $\pm 3\%$ for the sample with highest luminosity, and at most $\pm 1\%$ for the other samples. These effects were considered small and were not included in the plots of Figures 5 to 8.

In order to make the results easier to read, the upper limits on the λ couplings were also derived as a function of the sneutrino mass only. This was simply done by keeping the most conservative limit for each sneutrino mass, assuming $\Gamma_{\tilde{\nu}} > 150$ MeV/c^2. The

results can be seen in the same Figures as for the two-dimensional limits. The limits clearly show the centre-of-mass energy structure of the data samples; they are especially stringent for $M_{\tilde{\nu}} \simeq \sqrt{s}$.

5 Conclusion

The possibility of single production of supersymmetric particles was explored but none was seen. Upper limits at the 95% CL were derived in the mSUGRA constrained MSSM framework with low and high values of $\tan\beta$ for the two possible R_p violating couplings λ_{121} and λ_{131}. They are at the level of 2 to 3×10^{-3}, depending on $M_{\tilde{\nu}}$, when it is close to the centre-of-mass energy. They are slightly better for high $\tan\beta$ and slightly worse for λ_{131} as compared to λ_{121}. In any case, they are one or two orders of magnitude better than the published indirect limit, even for sneutrino masses outside the centre-of-mass energies of the analysed data, due to the t-channel and, more importantly, to the initial state radiation below the resonance.

Acknowledgements

We are greatly indebted to our technical collaborators, to the members of the CERN-SL Division for the excellent performance of the LEP collider, and to the funding agencies for their support in building and operating the DELPHI detector.
We acknowledge in particular the support of
Austrian Federal Ministry of Education, Science and Culture, GZ 616.364/2-III/2a/98,
FNRS–FWO, Flanders Institute to encourage scientific and technological research in the industry (IWT), Belgium,
FINEP, CNPq, CAPES, FUJB and FAPERJ, Brazil,
Czech Ministry of Industry and Trade, GA CR 202/99/1362,
Commission of the European Communities (DG XII),
Direction des Sciences de la Matière, CEA, France,
Bundesministerium für Bildung, Wissenschaft, Forschung und Technologie, Germany,
General Secretariat for Research and Technology, Greece,
National Science Foundation (NWO) and Foundation for Research on Matter (FOM), The Netherlands,
Norwegian Research Council,
State Committee for Scientific Research, Poland, SPUB-M/CERN/PO3/DZ296/2000, SPUB-M/CERN/PO3/DZ297/2000, 2P03B 104 19 and 2P03B 69 23(2002-2004)
JNICT–Junta Nacional de Investigação Científica e Tecnológica, Portugal,
Vedecka grantova agentura MS SR, Slovakia, Nr. 95/5195/134,
Ministry of Science and Technology of the Republic of Slovenia,
CICYT, Spain, AEN99-0950 and AEN99-0761,
The Swedish Natural Science Research Council,
Particle Physics and Astronomy Research Council, UK,
Department of Energy, USA, DE-FG02-01ER41155.

References

[1] H.P. Nilles, Phys. Rep. **110** (1984) 1;
H.E. Haber and G.L. Kane, Phys. Rep. **117** (1985) 75.

[2] P. Fayet, Phys. Lett. **B69** (1977) 489;
G. Farrar and P. Fayet, Phys. Lett. **B76** (1978) 575.

[3] S. Dimopoulos and L.J. Hall, Phys. Lett. **B207** (1988) 210.

[4] V. Barger et al., Phys. Rev. **D40** (1989) 2987.

[5] S. Katsanevas and P. Morawitz, Comput. Phys. Commun. **112** (1998) 227.

[6] H. Dreiner, in *Perspectives on Supersymmetry*, edited by G.L. Kane (World Scientific, Singapore, 1998) p. 462.

[7] R. Barate et al., ALEPH coll., Eur. Phys. J. **C12** (2000) 183;
P. Abreu et al., DELPHI coll., Phys. Lett. **B485** (2000) 45;
M. Acciarri et al., L3 coll., Phys. Lett. **B489** (2000) 81;
G. Abbiendi et al., OPAL coll., Eur. Phys. J. **C13** (2000) 553.

[8] P. Abreu et al., DELPHI coll., Nucl. Inst. and Meth. **A378** (1996) 57;
P. Aarnio et al., DELPHI coll., Nucl. Inst. and Meth. **A303** (1991) 233.

[9] F.A. Berends, P.H. Daverveldt and R. Kleiss, Comput. Phys. Commun. **40** (1986) 271.

[10] E. Accomando and A. Ballestrero, Comput. Phys. Commun. **99** (1997) 270;
E. Accomando, A. Ballestrero and E. Maina, hep-ph/0204052, to appear in Comput. Phys. Commun.

[11] S. Jadach, B.F.L. Ward and Z. Wąs, Comput. Phys. Commun. **130** (2000) 260.

[12] S. Jadach, W. Placzek and B.F.L. Ward, Phys. Lett. **B390** (1997) 298.

[13] S. Jadach, B.F.L. Ward and Z. Wąs, Comput. Phys. Commun. **79** (1994) 503.

[14] T. Sjöstrand, Comput. Phys. Commun. **39** (1986) 347.

[15] R. Keranen et al., Eur. Phys. J. direct **C7** (2000) 1.

[16] T. Sjöstrand, Comput. Phys. Commun. **82** (1994) 74.

[17] S. Catani et al., Phys. Lett. **B269** (1991) 432.

[18] P. Abreu et al., DELPHI coll., Eur. Phys. J. **C16** (2000) 371.

[19] V.F. Obraztsov, Nucl. Inst. and Meth. **A316** (1992) 388 and erratum **A399** (1997) 500.

[20] R.D. Cousins and V.L. Highland, Nucl. Inst. and Meth. **A320** (1992) 331.

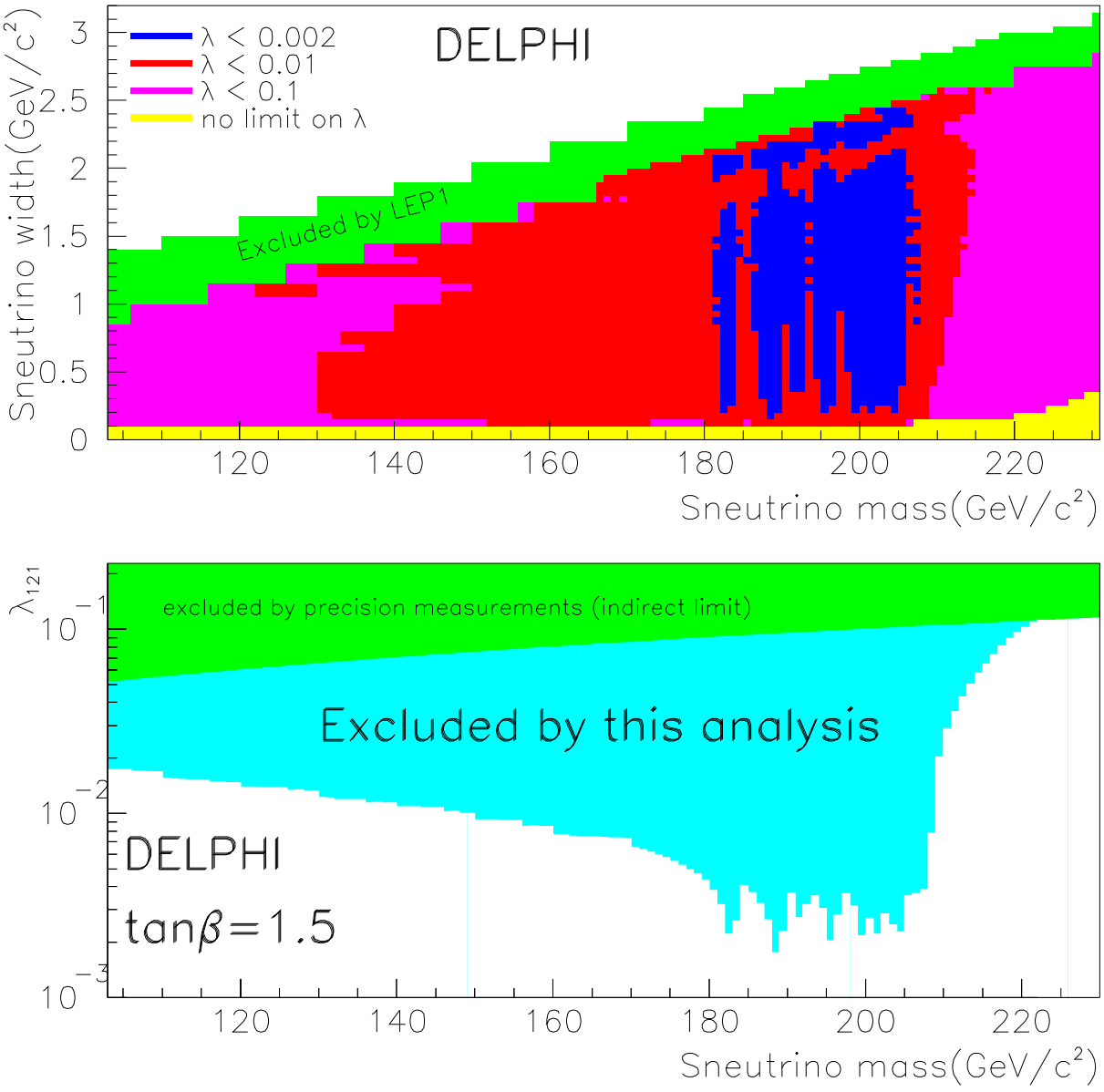

Figure 5: For $\tan\beta = 1.5$, upper limit on λ_{121} as a function of $M_{\tilde{\nu}}$ and $\Gamma_{\tilde{\nu}}$ (top) and as a function of $M_{\tilde{\nu}}$ assuming $\Gamma_{\tilde{\nu}} > 150$ MeV/c^2 (bottom). The white zone in the top plot corresponds to non existing sneutrino widths given the μ parameter range. The area entitled 'no limit on λ' corresponds to upper limits larger than 0.1. The indirect limit coming from precision measurements is drawn in the bottom plot assuming $M_{\tilde{e}_R} = M_{\tilde{\nu}}$.

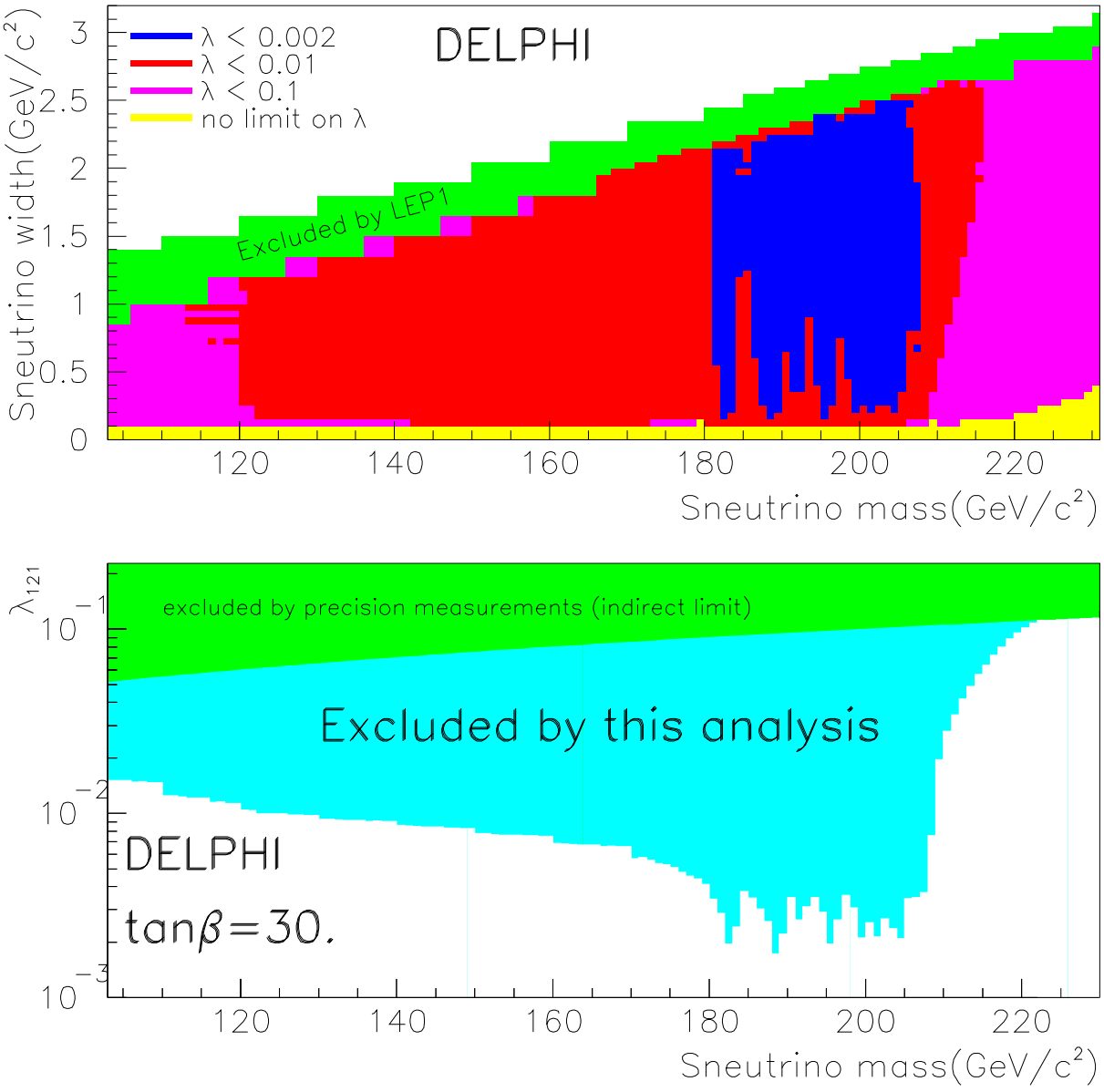

Figure 6: For $\tan\beta = 30$, upper limit on λ_{121} as a function of $M_{\tilde{\nu}}$ and $\Gamma_{\tilde{\nu}}$ (top) and as a function of $M_{\tilde{\nu}}$ assuming $\Gamma_{\tilde{\nu}} > 150$ MeV/c^2 (bottom). The white zone in the top plot corresponds to non existing sneutrino widths given the μ parameter range. The area entitled 'no limit on λ' corresponds to upper limits larger than 0.1. The indirect limit coming from precision measurements is drawn in the bottom plot assuming $M_{\tilde{e}_R} = M_{\tilde{\nu}}$.

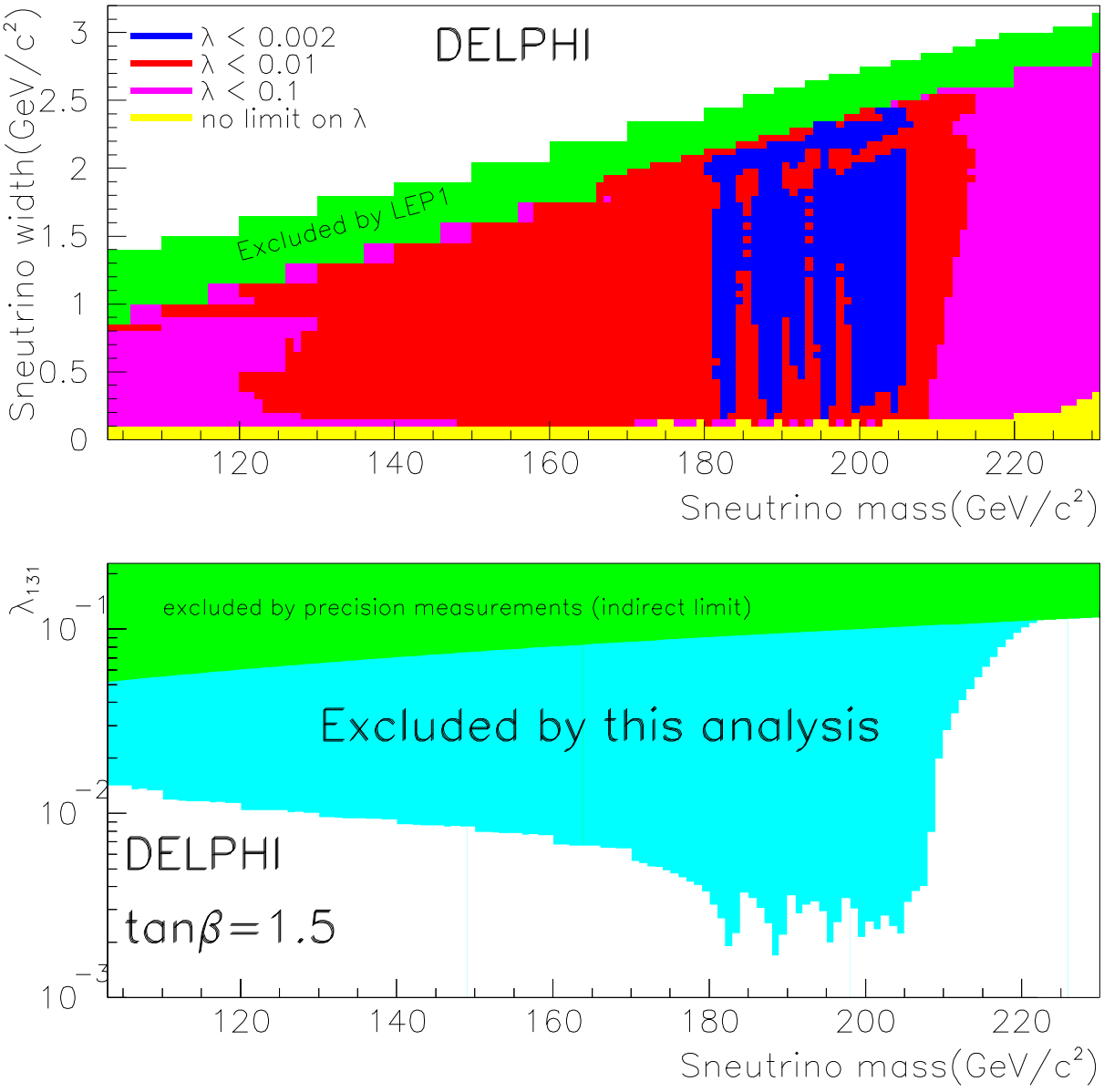

Figure 7: For $\tan\beta = 1.5$, upper limit on λ_{131} as a function of $M_{\tilde{\nu}}$ and $\Gamma_{\tilde{\nu}}$ (top) and as a function of $M_{\tilde{\nu}}$ assuming $\Gamma_{\tilde{\nu}} > 150$ MeV/c^2 (bottom). The white zone in the top plot corresponds to non existing sneutrino widths given the μ parameter range. The area entitled 'no limit on λ' corresponds to upper limits larger than 0.1. The indirect limit coming from precision measurements is drawn in the bottom plot assuming $M_{\tilde{e}_R} = M_{\tilde{\nu}}$.

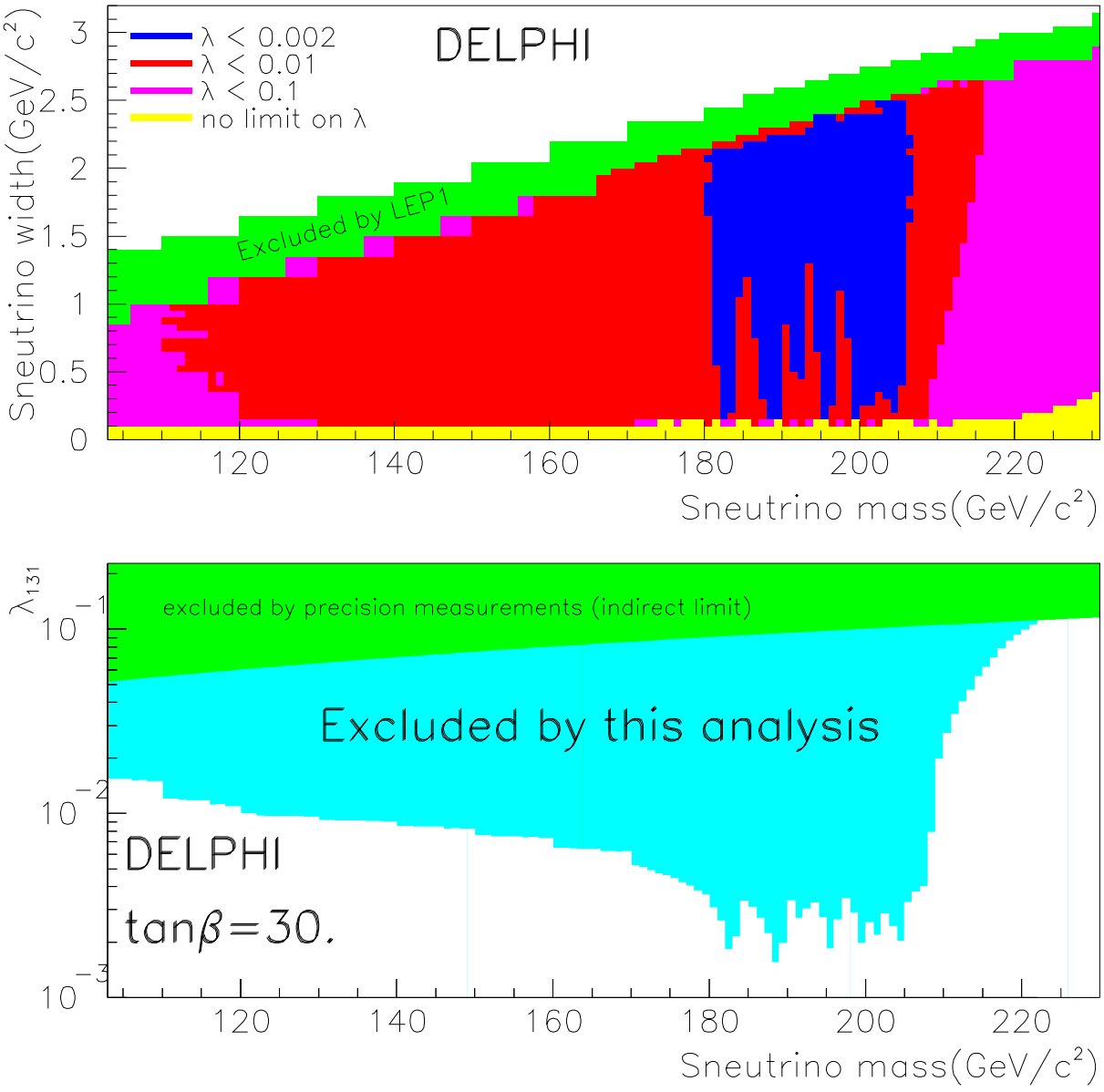

Figure 8: For $\tan\beta = 30$, upper limit on λ_{131} as a function of $M_{\tilde{\nu}}$ and $\Gamma_{\tilde{\nu}}$ (top) and as a function of $M_{\tilde{\nu}}$ assuming $\Gamma_{\tilde{\nu}} > 150$ MeV/c^2 (bottom). The white zone in the top plot corresponds to non existing sneutrino widths given the μ parameter range. The area entitled 'no limit on λ' corresponds to upper limits larger than 0.1. The indirect limit coming from precision measurements is drawn in the bottom plot assuming $M_{\tilde{e}_R} = M_{\tilde{\nu}}$.